

## Quantitative Analysis on the Validity of a Coarse-Grained Model for Nonequilibrium Polymeric Liquids under Flow

Chunggi Baig<sup>\*,†</sup> and Vagelis A. Harmandaris<sup>\*,‡,§</sup>

<sup>†</sup>Department of Chemical Engineering, University of Patras and FORTH-ICE/HT, Patras, GR 26504, Greece, <sup>‡</sup>Department of Applied Mathematics, University of Crete and FORTH-IACM, 71110 Heraklion, Greece, and <sup>§</sup>Max Planck Institute for Polymer Research, Ackermannweg 10, D-55128 Germany

Received January 13, 2010

Revised Manuscript Received February 19, 2010

Because of a very broad range of characteristic time and length scales of macromolecular fluids, a systematic hierarchical multiscale modeling approach is necessary to achieve a satisfactory description of the viscoelastic behavior of the system in various scales. Although widely used in the study of rheological properties of polymeric liquids under flow, atomistic nonequilibrium molecular dynamics (NEMD) simulations have been limited to rather short-chain polymeric materials due to the lack of computer capabilities confronting a very long relaxation behavior of long-chain polymers.<sup>1,2</sup> This limitation can be overcome by applying coarse-grained (CG) models which have proven to be very useful in the study of polymers with high molecular weights and with complicated structures at equilibrium.<sup>3,4</sup> In the past, Kröger<sup>5,6</sup> conducted NEMD studies of polymeric liquids using a simple bead–spring CG model, a well-known model for representing long polymeric systems at equilibrium.<sup>7</sup> Although still useful in the study of generic scaling properties, this ad hoc CG model lacks a link to a specific polymeric system and thus generally cannot be used for a direct quantitative comparison against experimental data. In an effort to relegate the disadvantage, systematic particle-based CG models for specific polymers have been proposed in the recent past.<sup>8–14</sup> These models are developed by lumping groups of chemically connected atoms into “superatoms” and deriving the effective, coarse-grained interaction potentials from the microscopic details of the atomistic models. Such CG models have shown to be very successful in predicting both structural and dynamical properties of long-chain polymeric systems at quiescent states; however, their predictive capabilities (both qualitatively and quantitatively) for rheological properties of polymeric systems under the application of an external flow field have not been assessed so far.

There are two main difficulties in the application of the CG models developed under equilibrium conditions to flowing polymeric systems. The first one is related to the distinct time scales between atomistic and CG models; that is, the time involved in the CG description generally does not correspond to the real physical time of the underlying chemistry in the original atomistic description. This is attributed to the softer effective interaction potentials between CG beads associated with the loss of degrees of freedom in the CG description.<sup>15</sup> While an ad hoc approach via an empirical time mapping between the atomistic and CG data has been introduced and shown to be quite successful to describe segmental and center-of-mass diffusion behaviors for equilibrium

systems,<sup>10,11</sup> its general validity for nonequilibrium systems has yet to be carefully analyzed, which is more important both practically and theoretically and thus dealt with in the present study. The second is associated with the variation of the effective CG force/potential field developed through representative structural properties (like pair distribution functions) with respect to the applied flow field.

Although there appeared a few works in the literature for studying nonequilibrium properties of polymers using specific CG particle models,<sup>13,14</sup> there have been until now no direct quantitative comparison between the atomistic and CG simulations of the polymeric system under flowing conditions. In this work we provide a detailed quantitative analysis of the overall predictive capabilities of a CG model for predicting the structural and dynamical properties by comparing between the atomistic and CG NEMD simulations for a representative polymeric system [atactic polystyrene (PS) melts] over a wide range of shear rates (covering both the linear and the highly nonlinear flow regime). The NEMD simulations have been based on a rigorous statistical mechanics algorithm, called the *p*-SLLOD algorithm<sup>2</sup> (which is the same as the original SLLOD algorithm<sup>16</sup> in the case of simple shear flow), alongside with the Lees–Edwards sliding-brick boundary conditions.<sup>17</sup> The well-known TraPPE united-atom (UA) force field<sup>18</sup> was used for the atomistic NEMD simulations of polystyrene melts and a recently developed coarse-grained model<sup>10</sup> (developed under equilibrium conditions) for the CG NEMD simulations. In this CG model each PS monomer is represented by two spherical superatoms: the first (CG bead “A”) corresponds to the CH<sub>2</sub> of a PS monomer plus the half mass of each of the two neighboring CH groups along the chain backbone, whereas the second (CG bead “B”) is just the phenyl ring. For more details about the CG model and the procedure to obtain the CG force field, we refer the readers to the original paper.<sup>10</sup>

A short PS melt with 10 repeat units per chain was adopted in this study. However, our methodology is general, and as shown elsewhere,<sup>11</sup> the present results from the short PS melt can be also applied to the polymeric system of high molecular weights by explicitly accounting for the effect of the density change due to the chain-end free volume effect. A total 45 and 120 molecules were employed for the atomistic and the CG simulation, respectively. Both systems were maintained at a temperature  $T = 463$  K and density  $\rho = 0.970$  g/cm<sup>3</sup> and were fully equilibrated before being subjected to flow. The set of the evolution equations (including also the equation for the Nosé–Hoover thermostat) was numerically integrated using *r*-RESPA (the reversible reference system propagator algorithm)<sup>19</sup> with two different time scales for an MD step: 2.39 and 0.48 fs for atomistic and 3.42 and 0.68 fs for CG simulations (note that, as mentioned above, the time in the CG model does not correspond to the real physical time). The response of the system was investigated over a broad range of strain rates corresponding to Weissenberg numbers ( $Wi$ ) in the interval  $0.4 \leq Wi \leq 200$ , covering both the linear and the highly nonlinear viscoelastic regime;  $Wi$  is defined as the product of the longest relaxation time  $\lambda$  of system at equilibrium (we found that  $\lambda = 1.1 \pm 0.05$  ns for the atomistic PS melt and  $\lambda = 0.22 \pm 0.01$  ns for the CG PS melt, as estimated by the integral below the stretched-exponential curve describing the autocorrelation function for the chain end-to-end vector) and the imposed shear rate. A sufficiently long simulation [e.g., up to 62 and 44 ns (corresponding to 26 million and 13 million MD steps) for the

\*To whom correspondence should be addressed: e-mail cbaig@iceht.forth.gr, Ph +30-2610-965219, Fax +30-2610-965223 (C.B.); e-mail vagelis@tem.uoc.gr, Ph +30-2810-393735 (V.H.).

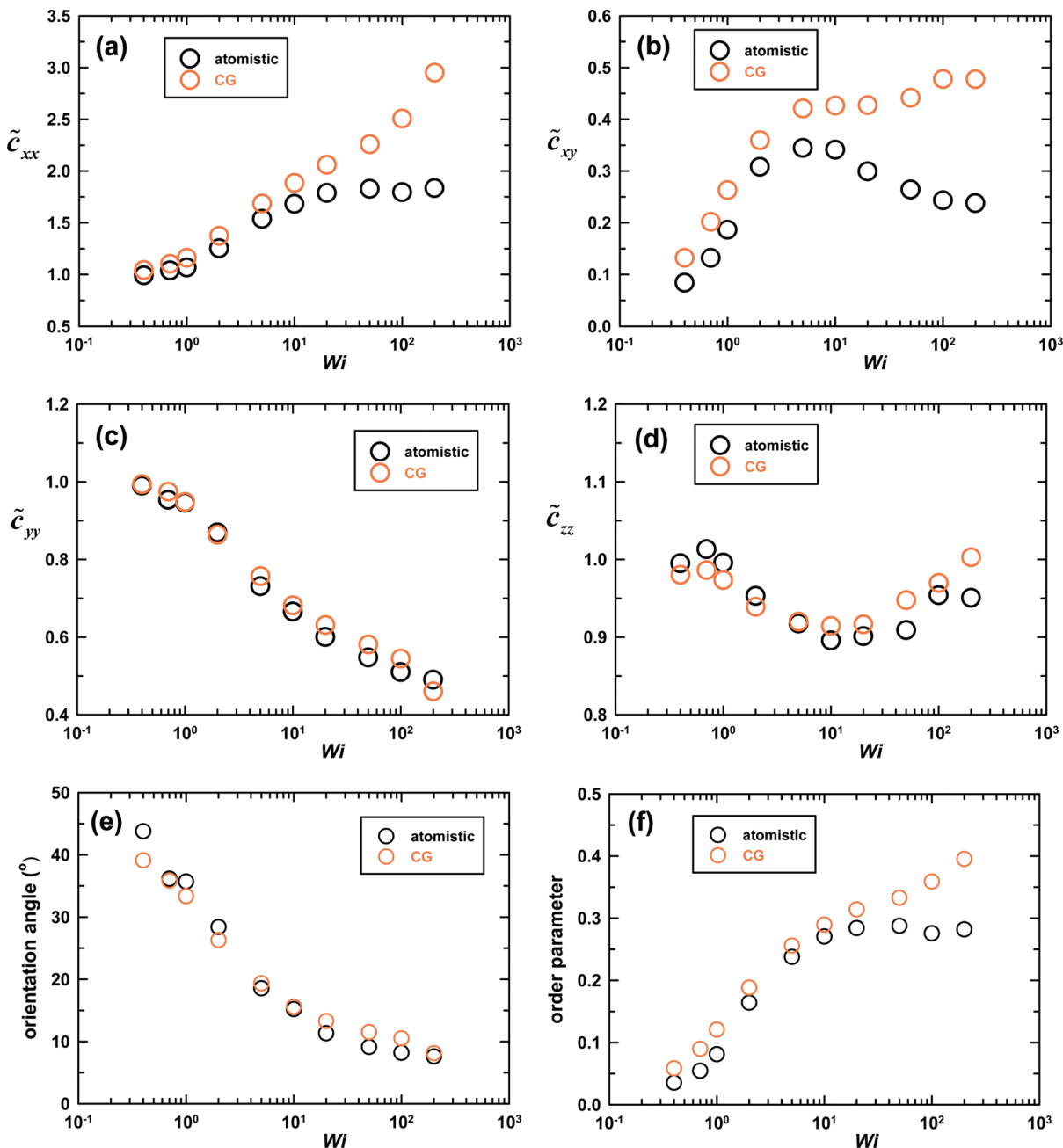


**Figure 1.** (a)–(d): Comparison of the conformation tensor as a function of  $Wi$  between the atomistic and CG NEMD simulations of the PS melt under shear. (e) The chain orientation angle and (f) order parameter based on the unit chain end-to-end vector are also presented. The error bars are smaller than the size of the symbols.

lowest shear rates in the atomistic and the CG simulation, respectively] was performed for each state point in order to reach steady-state and accumulate good statistics for physical properties.

We study first the structural and conformational properties of the PS melt and how they are compared between the atomistic and the CG simulation as a function of the imposed shear rate. Figure 1 presents the results for the conformation tensor  $\tilde{\mathbf{c}}$  whose components are defined as  $\tilde{c}_{\alpha\beta} \equiv 3\langle R_\alpha R_\beta \rangle / \langle R^2 \rangle_{\text{eq}}$  ( $\alpha, \beta = x, y, z$ ) with  $\mathbf{R}$  being the chain end-to-end vector and the subscript eq denoting equilibrium conditions. First of all, for all the four components ( $\tilde{c}_{xx}$ ,  $\tilde{c}_{xy}$ ,  $\tilde{c}_{yy}$ , and  $\tilde{c}_{zz}$ ), the predictions of the CG model are seen to be quantitatively in good agreement with the atomistic results at low-to-intermediate shear rates (i.e.,  $Wi \leq 5$ ); however, a significant discrepancy develops upon further increasing the shear rate, notably observed for  $\tilde{c}_{xx}$  and  $\tilde{c}_{xy}$ . Specifically, for  $\tilde{c}_{xx}$  the atomistic model predicts a monotonic increase up to

$Wi \approx 50$  at which an asymptotic value ( $\sim 1.83$ ) is attained. By comparison, the CG model is observed to conform very well to the atomistic model up to  $Wi \approx 5$ , beyond which it, however, predicts a further increase of  $\tilde{c}_{xx}$  with increasing the flow strength.

This result implicates some key features of the CG model (these are further considered as generic to most coarse-grained models). First, the asymptotic behavior of  $\tilde{c}_{xx}$  displayed by the atomistic model is attributed to two effects: (a) finite chain extensibility due to the strong bond-stretching and bond-bending interactions between neighboring atoms along the chain, which limits the maximum extension of the molecules, and (b) chain rotation occurring in shear flow, which precludes the molecules from possessing a fully stretched conformation (i.e., *all-trans* conformation). Although these two effects are exposed in both the atomistic and CG models, there is a quantitative difference in their effects on the structure; in the CG model, each bead represents

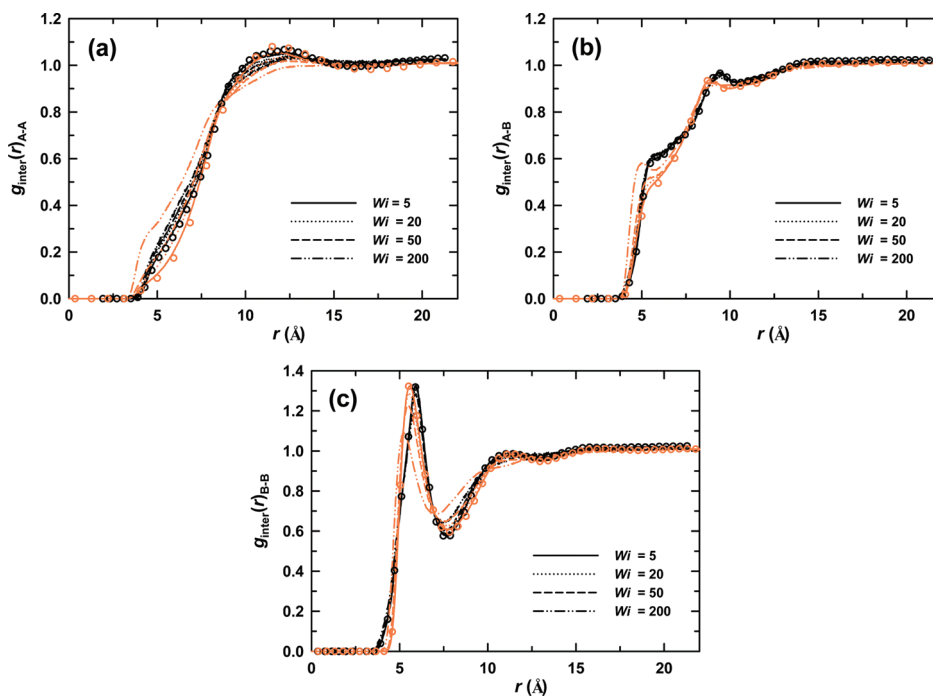


**Figure 2.** Intermolecular pair distribution function  $g_{\text{inter}}(r)$  for (a) A–A, (b) A–B, and (c) B–B beads at four different  $Wi$  numbers. The black and orange colors represent the atomistic and CG results, respectively. The circles represent  $g_{\text{inter}}(r)$  at equilibrium states.

several atoms, which renders relatively weaker energies for the bond-stretching and bond-bending interactions between neighboring beads and thus allows for a larger maximum chain extension than the atomistic model (as is evident in Figure 1a). Furthermore, the “effective” bead friction in response to flow may vary (e.g., typically increases) with the flow strength, since the local chain structure is generally not to be the same between the atomistic and the CG model under the same flow conditions (this feature will be further discussed later in regard to diffusion phenomena). Consequently, the CG chains are expected to be quantitatively more affected by an external field, especially at strong fields where the local bonded structure of the chains and the effective bead friction coefficient can change significantly.

Such large chain deformations exhibited in the CG model at high values of the  $Wi$  number are further reflected for the  $xy$  component of the conformation tensor, as presented in Figure 1b. The overall change of  $\tilde{c}_{xy}$  with respect to the shear rate can be understood by considering two competing effects: (a) spatial correlation between the  $x$  and  $y$  components of the chain end-to-end vector, leading to an increase of  $\tilde{c}_{xy}$  (this effect can be further enhanced by chain stretching), and (b) chain orientation along the flow direction, leading to a decrease of  $\tilde{c}_{xy}$ . The competition between these two effects may thus give rise to a plateau (e.g., the CG data in Figure 1b) or maximum (e.g., the atomistic data in Figure 1b and those of polyethylene melts<sup>20</sup>) of  $\tilde{c}_{xy}$  at an intermediate shear rate. Overall, much larger enhancement of  $\tilde{c}_{xy}$  is observed in the CG model compared to the atomistic model, especially at high flow fields where significantly larger chain deformations of the CG chains occur, as shown in  $\tilde{c}_{xx}$ .

Interestingly, very good agreement between the atomistic and the CG model is observed for  $\tilde{c}_{yy}$  in the whole range of shear rates, indicating that the CG model predicts reliably the degree of chain orientation in both linear and highly nonlinear flow regimes. This excellent capability of the CG model is also seen for  $\tilde{c}_{zz}$  as plotted in Figure 1d, where the overall, highly nonlinear behavior of  $\tilde{c}_{zz}$  exhibited in the atomistic result is reproduced remarkably well by the CG model (incidentally, the minimum occurring at  $Wi \approx 10$  is thought to be caused by large dynamical perturbations which

enhance an elastic recoiling of the molecules in the neutral ( $z$ -) direction).

Overall, the CG model developed through a systematic procedure under equilibrium conditions appears to be in quantitatively reasonable agreement with the atomistic model at low-to-intermediate flow fields. However, the limited capability of the CG model for predicting  $\tilde{c}_{xx}$  and  $\tilde{c}_{xy}$ , which is in sharp contrast with the excellent predictions for  $\tilde{c}_{yy}$  and  $\tilde{c}_{zz}$  in the entire flow regime, indicates that we should be very circumspect when assessing a coarse-grained model for its predictive capabilities by looking into as many physical quantities as possible; for instance, in contrast to the accurate prediction for the chain orientation angle in the whole range of  $Wi$  numbers (Figure 1e), the CG model showed only a limited applicability (i.e.,  $Wi \leq 10$ ) for the associated order parameter (Figure 1f).

Further detailed information on the liquid structure is obtained by looking into the pair correlation function  $g(r)$ . Figure 2 displays the intermolecular part of  $g(r)$  for three different pairs in terms of the coarse-grained beads: (a) A–A, (b) A–B, and (c) B–B. First, at equilibrium state (denoted by circles), the CG plot for each pair is seen to be in reasonable agreement with the atomistic one. Under flowing conditions, as the field strength is increased, the atomistic model exhibits (i) an increase of  $g_{\text{inter}}(r)_{\text{A–A}}$  below  $r \approx 8.5$  Å and its decrease in the region around the first peak ( $8.5$  Å  $< r < 14$  Å), (ii) a slight increase of  $g_{\text{inter}}(r)_{\text{A–B}}$  below  $r \approx 5.5$  Å and a diminished magnitude of the main peak at  $r \approx 9.4$  Å, and (iii) overall shift of  $g_{\text{inter}}(r)_{\text{B–B}}$  to the left together with the reduced maximum at  $r \approx 5.9$  Å and the reduced minimum at  $r \approx 7.7$  Å. As regards the phenomenon i for  $g_{\text{inter}}(r)_{\text{A–A}}$ , while the CG model is shown to predict correctly the overall trends, it appears to largely overestimate the variation. This excessive prediction of the CG model is supposed to come from relatively weak excluded volume interactions between the CG beads compared to those of between the original atoms; this feature of the CG model gets more influential with increasing the flow strength, since the intermolecular interactions (or collisions) between the beads become more intensified. Further effects are ascribed to a built-in large flexibility of CG molecules via the applied coarse-graining procedure, leading to larger deformations

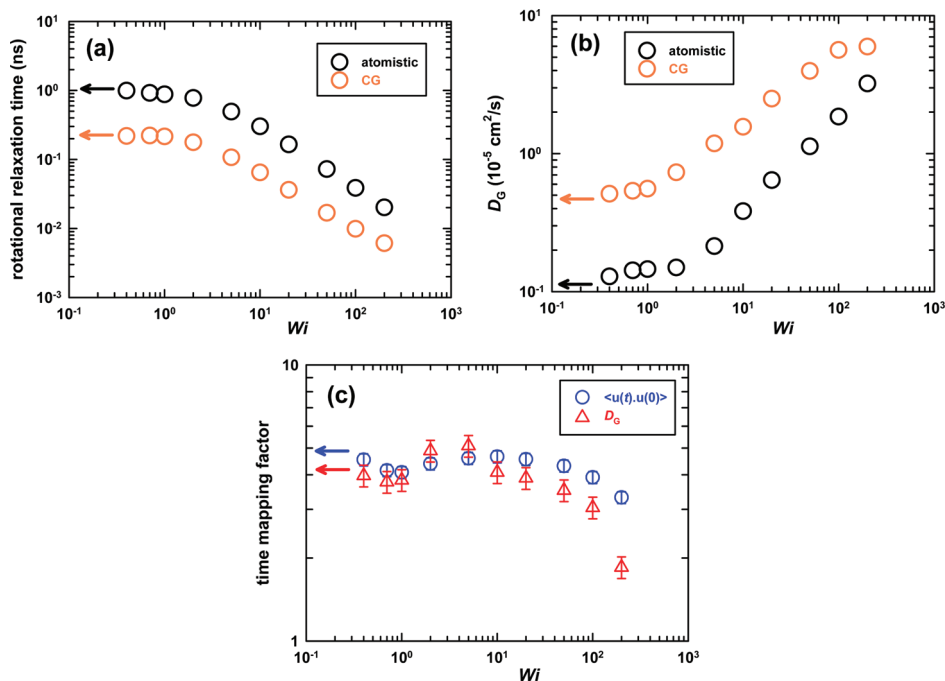


**Figure 3.** Variation of (a) the rotational relaxation time calculated by the decay of the autocorrelation function  $\langle \mathbf{u}(t) \cdot \mathbf{u}(0) \rangle$  of the unit chain end-to-end vector  $\mathbf{u}(t)$  and (b) the chain center-of-mass diffusion coefficient  $D_G$  as a function of  $Wi$ . The error bars are smaller than the size of the symbols. In (c) we present the time mapping factor as a function of  $Wi$  obtained by matching the CG data with the corresponding atomistic ones for the relaxation time and  $D_G$ . The arrows represent their values at equilibrium states.

of the CG chains than the atomistic ones in response to flow (as was seen in Figure 1). Qualitatively similar behaviors are also observed in the case of  $g_{\text{inter}}(r)_{A-B}$  (Figure 2b) and  $g_{\text{inter}}(r)_{B-B}$  (Figure 2c). We further report (results not shown here) that the CG model predicts correctly only little changes of  $g_{\text{inter}}(r)$  for all the pairs at small shear rates ( $Wi < 5$ ), as completely consistent with the atomistic model. Overall, for  $Wi > 5$ , the CG model is found to predict qualitatively well the general trend of the structural changes as a function of the flow strength, but quantitatively it overestimates them due to its relatively weak excluded volume interactions and large chain flexibility.

We now turn our attention to the predictive capabilities of the CG model for dynamical properties. As mentioned earlier, due to the reduced effective hydrodynamic friction of CG beads, the time in the CG description does not correspond to the real physical time (in general, CG dynamics is to be faster than the physical atomistic one). Unfortunately, it is highly intractable to give analytical predictions for the time mapping factor and its variation under flow due to a strongly fluctuating, complex local energy landscape. A semiempirical way to relieve this limitation is by performing a “scaling” of the CG time using dynamical data taken from experiments or atomistic simulations. An important question here is whether or not the time mapping factor based on a dynamical quantity is to be consistent with that of other dynamical quantities. To this, we examined translational and orientational motions of the polymer chains. In Figure 3a we plot the variation of the rotational (longest) relaxation time of the system with the imposed flow rate, as obtained by measuring the autocorrelation function of the chain end-to-end vector. It is quite remarkable to see the overall consistency between the atomistic and the CG model in their predictions for the effects of the flow field on the relaxation time in the whole range of shear rates. Comparing with the atomistic results, we mention specifically that (i) the CG model predicts correctly the small variations of the relaxation time occurring at low strain rates ( $Wi < 1$ ), (ii) it also predicts correctly the incipient flow strength (i.e.,  $Wi \approx 2$ ) beyond which a large decrease of the relaxation time follows,

(iii) it further predicts (quantitatively) very well the fractional changes of the relaxation time up to an intermediate flow rate ( $Wi \approx 10$ ), but (iv) it underestimates the decrease of the relaxation time with increasing  $Wi$  at high flow regime ( $Wi > 10$ ). Quantitatively similar behaviors are found for the center-of-mass diffusion coefficient ( $D_G$ ) of molecules, as plotted in Figure 3b (purely convective contributions from the applied strain rate were excluded in these calculations, as suggested by Moore et al.<sup>21</sup>); the CG model reproduces satisfactorily the atomistic results such as very small changes (within statistical uncertainties) of  $D_G$  under weak flow fields, a large increase of  $D_G$  beyond  $Wi \approx 2$ , but it again underestimates the change of  $D_G$  at strong flow fields ( $Wi > 10$ ) compared to the atomistic result. It is thus concluded that if the flow strength (based on  $Wi$ ) is properly rescaled by the time scale based on the relaxation time obtained under equilibrium conditions, the CG model is capable of predicting reasonably well the dynamic properties of the system at low-to-intermediate strain rates (e.g.,  $Wi < 10$ ), beyond which it tends to underestimate their changes with respect to the flow strength.

From a physical point view, it is quite instructive to associate the underestimation of the CG model at strong flow fields with the variation of the effective friction coefficient of CG beads. Since the larger bead friction would lead to the slower relaxation and diffusion of the chains, the above result indicates that the effective bead friction increases with the field strength at strong flow fields. The physical origin underlying this increase of the bead friction can be ascribed to an effective increase of chain stiffness under strong fields, as the CG chains become much more deformed (stretched) than the atomistic ones (as was evident in Figure 1a) at the same values of  $Wi$ ; furthermore, the larger extension of CG chains facilitates the dynamical interactions between the molecules and therefore leads to a slowdown of both chain rotation (thus increasing the relaxation time) and chain translation (thus decreasing  $D_G$ ).

Lastly, in Figure 3c we plot the two time mapping factors [one based on the relaxation time (Figure 3a) and another based on  $D_G$  (Figure 3b)] obtained by empirically matching the CG results

with the corresponding atomistic ones in the long time regime. Despite rather complicated (nonmonotonic) variation of the mapping curves with respect to  $Wi$ , the overall behaviors appear to be consistent with each other in the whole flow regime (although the time mapping factor based on  $D_G$  appears to be more fluctuating than that based on the relaxation time). In more detail, the two mapping factors are found to be quantitatively quite similar to each other at low-to-intermediate flow regime (i.e.,  $Wi < 10$ ), beyond which the time mapping factor based on  $D_G$  drops more rapidly than that based on the relaxation time (this seems to indicate that the variation of the bead friction is more effective in chain translation than chain rotation). Since it is a highly nontrivial problem to predict theoretically the effects of a coarse-graining and the concomitant entropy loss and introduction of dissipation on the system dynamics in response to an external field, the results presented here are considered to be very informative both practically and theoretically for the future application and development of a coarse-grained model.

In conclusion, we carried out a detailed analysis to assess the validity of a systematic CG model describing polystyrene melts at equilibrium for the melts at nonequilibrium states under shear flow. By studying both structural and dynamical properties with respect to the shear rate, we found that the large-scale chain conformation is reasonably well predicted by the CG model up to an intermediate flow strength ( $Wi < 10$ ), beyond which, however, a significant discrepancy between the atomistic and the CG models develops; this has been attributed to excessively large chain deformations allowed in the CG model due to relatively weak potential energies for local bonded interactions between CG beads. Also, the CG model appeared to predict correctly the overall change of the liquid structure as a function of the shear rate; however, it overestimated the variation due to relatively weak excluded volume interactions between CG beads and large chain flexibility. Furthermore, the CG model was found to predict reasonably well the dynamical properties (the relaxation time and  $D_G$ ) at low-to-intermediate strain rates, beyond which it underestimated their variations with the flow strength; this has been ascribed to an increase of the effective bead friction coefficient at strong flow fields associated with an increase of chain stiffness and chain extension.

Finally, as shown in ref 11, by explicitly accounting for the effect of density increase (decrease of available free volume) of system with increasing the chain length, it is possible to estimate, in a reasonable accuracy, the dynamical properties (e.g., diffusion coefficient, time mapping factor, etc.) of long-chain PS melts via the CG MD simulations of a short-chain PS melt with the density correction at equilibrium. Under flowing conditions, although it is not perfectly clear at present whether the effects of the density change associated with the variation of chain length on the structural and dynamical properties would be quantitatively the same as those observed under equilibrium conditions, we conjecture that the overall trends on the structural and dynamical behaviors of the short PS melt with respect to the flow strength found in this work are likely to be applicable to long (entangled) PS melts in a quantitative manner if the flow strength is expressed in terms of the  $Wi$  number. We further point out that the time rescaling issue shown in this study can be directly related to and be partly resolved via a systematic force-field rescaling procedure.

On the basis of the present results, we would mention as a general guideline that the particle-based CG models developed using systematic approaches with respecting the original atomic chemistry are capable of predicting both structural and dynamical properties quantitatively in a reasonable accuracy at low-to-intermediate values of the  $Wi$  numbers, beyond which the predictive capabilities of the CG models would be largely deteriorate. In this regard, general theoretical developments of estimating (even approximately) the dynamic time-mapping characteristic with respect to the structure and degree of coarse-graining would be invaluable. We hope the information presented here to be useful as guidance in assessing rheological properties produced by a coarse-grained model in practical applications.

**Acknowledgment.** Partial support of this work was provided by the National Science Foundation under Grant CBET-0742679 through the resources of the PolyHub Virtual Organization.

## References and Notes

- (1) Evans, D. J.; Morriss, G. P. *Statistical Mechanics of Nonequilibrium Liquids*; Academic Press: New York, 1990.
- (2) (a) Baig, C.; Edwards, B. J.; Keffer, D. J.; Cochran, H. D. *J. Chem. Phys.* **2005**, *122*, 184906. (b) Baig, C.; Edwards, B. J.; Keffer, D. J.; Cochran, H. D.; Harmandaris, V. A. *J. Chem. Phys.* **2006**, *124*, 084902.
- (3) *Monte Carlo and Molecular Dynamics Simulations in Polymer Science*; Binder, K., Ed.; Oxford University Press: New York, 1995.
- (4) *Coarse-Graining of Condensed Phase and Biomolecular Systems*; Voth, G. A., Ed.; Chapman and Hall: London, 2008.
- (5) Kröger, M.; Hess, S. *Phys. Rev. Lett.* **2000**, *85*, 1128.
- (6) Kröger, M. *Phys. Rep.* **2004**, *390*, 453.
- (7) Kremer, K.; Grest, G. S. *J. Chem. Phys.* **1990**, *92*, 5057.
- (8) Tschöp, W.; Kremer, K.; Batoulis, J.; Buerger, T.; Hahn, O. *Acta Polym.* **1998**, *49*, 61; **1998**, *49*, 75.
- (9) Reith, D.; Meyer, H.; Müller-Plathe, M. *Macromolecules* **2001**, *34*, 2335.
- (10) Harmandaris, V. A.; Reith, D.; Van der Vegt, N. F. A.; Kremer, K. *Macromol. Chem. Phys.* **2007**, *208*, 2109.
- (11) (a) Harmandaris, V. A.; Kremer, K. *Macromolecules* **2009**, *42*, 791. (b) *Soft Matter* **2009**, *5*, 3920.
- (12) Padding, J. T.; Briels, W. J. *J. Chem. Phys.* **2002**, *117*, 925.
- (13) Padding, J. T.; Briels, W. J. *J. Chem. Phys.* **2003**, *118*, 10276.
- (14) (a) Chen, X.; et al. *Macromolecules* **2007**, *40*, 8047. (b) *Phys. Chem. Chem. Phys.* **2009**, *11*, 1977.
- (15) In the coarse-grained MD simulations with CG models which are very close to the real chemistry, like the one used in this work, the real friction is usually not included because (a) the degree of coarse-graining is not too large and thus maintains a reasonable accuracy close to the atomistic model and (b) it is generally not feasible to estimate accurately the friction coefficient a priori due to the insufficient time-scale separation between the atomistic and CG descriptions. In contrast, for coarser CG models where there is a clear separation of time scales between the atomistic and CG descriptions, physical friction forces can be explicitly taken into account in the equations of motion, as there have been a few works; see, for example, ref 12.
- (16) Evans, D. J.; Morriss, G. P. *Phys. Rev. A* **1984**, *30*, 1528.
- (17) Lees, A. W.; Edwards, S. F. *J. Phys. C* **1972**, *5*, 1921.
- (18) Martin, M. G.; Siepmann, J. I. *J. Phys. Chem. B* **1999**, *103*, 4508.
- (19) Tuckerman, M.; Berne, B. J.; Martyna, G. J. *J. Chem. Phys.* **1992**, *97*, 1990.
- (20) Kim, J. M.; Keffer, D. J.; Kröger, M.; Edwards, B. J. *J. Non-Newtonian Fluid Mech.* **2008**, *152*, 168.
- (21) Moore, J. D.; Cui, S. T.; Cochran, H. D.; Cummings, P. T. *J. Non-Newtonian Fluid Mech.* **2000**, *93*, 83.